Inorganic Chemistry

Article

pubs.acs.org/IC

New Alkali-Metal Gallium Selenites, $AGa(SeO_3)_2$ (A = Li, Na, K, and Cs): Effect of Cation Size on the Framework Structures and Macroscopic Centricities

Dong Woo Lee and Kang Min Ok*

Department of Chemistry, Chung-Ang University, 221 Heukseok-dong, Dongjak-gu, Seoul 156-756, Republic of Korea

Supporting Information

ABSTRACT: New quaternary alkali-metal gallium selenites, $AGa(SeO_3)_2$ (A = Li, Na, K, and Cs), have been synthesized through hydrothermal reactions. Single-crystal X-ray diffraction has been used to determine the structures of the reported materials. The stoichiometrically equivalent materials crystallize in three-dimensional framework structures and share a similar bonding network that is composed of distorted GaO_6 octahedra and asymmetric SeO_3 polyhedra. However, all four materials exhibit different framework geometries attributable to the size of the alkali-metal cations and the orientation of lone pairs on Se^{4+} cations. Macroscopic centricities of the materials are also affected by interactions between the cation and the oxide ligands on GaO_6 and SeO_3 groups. Complete characterization including infrared spectroscopy, elemental analyses, thermal analyses, dipole moment calculations, and second-harmonic generation properties for the compounds is also presented.

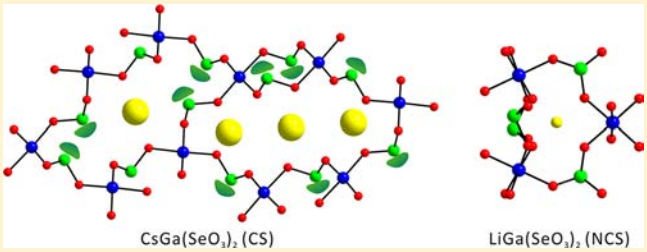

INTRODUCTION

Metal selenites, i.e., oxide materials containing a Se^{4+} cation, have been of great interest to inorganic materials chemists because of their local asymmetric coordination environments with the stereoactive lone pairs. Combining locally unsymmetrical coordination moieties, in fact, has been considered to be an effective method for generating macroscopic noncentrosymmetry (NCS) in any material.[1] Since the NCS materials can exhibit particular kinds of superior performing functional properties such as second-harmonic generation (SHG), piezoelectricity, pyroelectricity, and ferroelectricity, demand for discovering technologically important materials remains extremely strong.[2] With oxide materials, the lone pairs creating an asymmetric coordination environment are thought to be the result of a second-order Jahn−Teller (SOJT) distortion.[3] Although the local asymmetric units are necessary, however, it should be noted that they are not sufficient condition for creating crystallographic NCS. In other words, many compounds with extended structures may crystallize in centrosymmetric structures once the acentric units are aligned in an antiparallel manner. Therefore, it would be crucial to understand factors controlling the macroscopic symmetry in order to rationally discover new NCS materials.[4] A few important factors that may contribute to determine the materials' overall centricities include the size of metal cations, the hydrogen bond, and the framework flexibility.[5] In addition, once the asymmetric coordination environment of the lone pair cations is combined with other flexible cations such as p elements, much richer structural chemistry can also be expected from the materials. Recently, we reported a new family of quaternary alkali-metal indium selenites materials, $AIn(SeO_3)_2$ (A = Na, K, Rb, and Cs), and demonstrated that the size of alkali-metal cations significantly influences the framework structures.[6] Now we replaced the p element to the cation with different framework flexibility, Ga^{3+} in a new quaternary gallium selenite system. Thus far, several gallium selenites or tellurites materials in a highly asymmetric coordination environment have been reported,[7] and $Ga_2(SeO_3)_3(H_2O)_3$[7b] and α-$Ga_2(TeO_3)_3$[7g] crystallized in the NCS crystal structure. Herein, we report hydrothermal syntheses and characterization of a new series of alkali-metal gallium selenites, $AGa(SeO_3)_2$ (A = Li, Na, K, and Cs). We will demonstrate how the size of alkali-metal cations influences the framework structures as well as the macroscopic centricities in the stoichiometrically equivalent materials. With the NCS $LiGa(SeO_3)_2$, SHG properties will also be presented.

EXPERIMENTAL SECTION

Reagents. Li_2CO_3 (Hayashi, 98.0%), Na_2CO_3 (Hayashi, 99.5%), K_2CO_3 (Jin Chemical, 99.5%), Cs_2CO_3 (Aldrich, 99.0%), Ga_2O_3 (Alfa Aesar, 99.999%), $Ga(NO_3)_3{\cdot}xH_2O$ (Alfa Aesar, 99.9%), and SeO_2 (Aldrich, 98%) were used as received.

Synthesis. Pure phase crystals of $AGa(SeO_3)_2$ (A = Li, Na, K, and Cs) were prepared by hydrothermal reactions. For $LiGa(SeO_3)_2$, 0.111 g (1.50×10^{-3} mol) of Li_2CO_3, 0.128 g (5.00×10^{-4} mol) of $Ga(NO_3)_3{\cdot}xH_2O$, 0.222 g (2.00×10^{-3} mol) of SeO_2, and 1 mL of deionized water were combined. For $NaGa(SeO_3)_2$, 0.318 g (3.00×10^{-3} mol) of Na_2CO_3, 0.256 g (1.00×10^{-3} mol) of $Ga(NO_3)_3{\cdot}xH_2O$, 0.444 g (4.00×10^{-3} mol) of SeO_2, and 2 mL of deionized water were combined. For $KGa(SeO_3)_2$, 0.415 g (3.00×10^{-3} mol) of K_2CO_3,

Received: January 8, 2013
Published: April 16, 2013

 © 2013 American Chemical Society dx.doi.org/10.1021/ic400458a | Inorg. Chem. 2013, 52, 5176−5184

Table 1. Crystallographic Data for $AGa(SeO_3)_2$ (A = Li, Na, K, and Cs)

formula	$LiGaSe_2O_6$	$NaGaSe_2O_6$	$KGaSe_2O_6$	$CsGaSe_2O_6$
fw	330.58	346.63	362.74	456.55
space group	*I*-42*d* (No. 122)	*Pnma* (No. 62)	*Pnma* (No. 62)	*C*2/*m* (No. 12)
a (Å)	10.5402(15)	12.4545(2)	14.9753(3)	13.7906(7)
b (Å)	10.5402(15)	5.29670(10)	5.32510(10)	5.4755(3)
c (Å)	9.828(2)	7.80440(10)	7.28750(10)	18.3055(9)
β (deg)	90	90	90	107.612(2)
V (Å^3)	1091.8(3)	514.839(14)	581.141(18)	1317.47(12)
Z	8	4	4	8
T (K)	173.0(2)	173.0(2)	173.0(2)	173.0(2)
λ (Å)	0.71073	0.71073	0.71073	0.71073
ρ_{calcd} (g cm^{-3})	4.022	4.472	4.146	4.604
μ (mm^{-1})	18.330	19.525	17.941	20.643
$R(F)^a$	0.0223	0.0292	0.0182	0.0320
$R_w(F_o^2)^b$	0.0473	0.0636	0.0386	0.0765
Flack parameter	−0.02(3)	N/A	N/A	N/A

$^aR(F) = \Sigma\ ||F_o| - |F_c||/\Sigma|F_o|$. $^bR_w(F_o^2) = [\Sigma w(F_o^2 - F_c^2)^2/\Sigma w(F_o^2)^2]^{1/2}$.

Table 2. Selected Bond Distances (Angstroms) for $AGa(SeO_3)_2$ (A = Li, Na, K, and Cs)

	bond distances	bond valence		bond distances	bond valence
$LiGa(SeO_3)_2$			$NaGa(SeO_3)_2$		
Ga(1)−O(1) × 2	1.991(3)	0.479	Ga(1)−O(1)	1.925(4)	0.590
Ga(1)−O(2) × 2	1.974(3)	0.501	Ga(1)−O(2) × 2	1.990(3)	0.495
Ga(1)−O(3) × 2	1.955(3)	0.527	Ga(1)−O(3)	1.968(4)	0.526
bond valence sum of Ga(1)		3.014	Ga(1)−O(4) × 2	1.993(3)	0.491
Se(1)−O(1)	1.702(3)	1.260	bond valence sum of Ga(1)		3.088
Se(1)−O(2)	1.706(3)	1.251	Se(1)−O(1)	1.678(4)	1.433
Se(1)−O(3)	1.682(3)	1.323	Se(1)−O(2) × 2	1.694(3)	1.372
bond valence sum of Se(1)		3.834	bond valence sum of Se(1)		4.177
			Se(2)−O(3)	1.695(4)	1.368
			Se(2)−O(4) × 2	1.693(3)	1.376
			bond valence sum of Se(2)		4.120
	$KGa(SeO_3)_2$			$CsGa(SeO_3)_2$	
Ga(1)−O(1)	1.997(2)	0.486	Ga(1)−O(1)	2.030(9)	0.444
Ga(1)−O(2) × 2	2.0181(15)	0.459	Ga(1)−O(2) × 2	1.943(6)	0.562
Ga(1)−O(3)	1.956(2)	0.543	Ga(1)−O(3) × 2	2.037(6)	0.436
Ga(1)−O(4) × 2	1.9737(16)	0.517	Ga(1)−O(6)	1.961(8)	0.536
bond valence sum of Ga(1)		2.981	bond valence sum of Ga(1)		2.976
Se(1)−O(1)	1.697(2)	1.361	Ga(2)−O(4)	1.954(9)	0.546
Se(1)−O(2) × 2	1.6929(16)	1.376	Ga(2)−O(5) × 2	1.990(6)	0.495
bond valence sum of Se(1)		4.113	Ga(2)−O(7) × 2	2.026(5)	0.449
Se(2)−O(3)	1.700(2)	1.350	Ga(2)−O(8)	2.020(9)	0.457
Se(2)−O(4) × 2	1.6928(17)	1.376	bond valence sum of Ga(2)		2.891
bond valence sum of Se(2)		4.102	Se(1)−O(1)	1.715(8)	1.296
			Se(1)−O(2) × 2	1.696(6)	1.365
			bond valence sum of Se(1)		4.026
			Se(2)−O(3) × 2	1.692(6)	1.379
			Se(2)−O(4)	1.691(9)	1.383
			bond valence sum of Se(2)		4.141
			Se(3)−O(5) × 2	1.695(6)	1.368
			Se(3)−O(6)	1.702(8)	1.343
			bond valence sum of Se(3)		4.079
			Se(4)−O(7) × 2	1.713(5)	1.303
			Se(4)−O(8)	1.710(8)	1.314
			bond valence sum of Se(4)		3.920

0.256 g (1.00 × 10^{-3} mol) of $Ga(NO_3)_3{\cdot}xH_2O$, 0.444 g (4.00 × 10^{-3} mol) of SeO_2, and 1 mL of deionized water were combined. For $CsGa(SeO_3)_2$, 0.488 g (3.00 × 10^{-3} mol) of Cs_2CO_3, 0.128 g (5.00 × 10^{-4} mol) of $Ga(NO_3)_3{\cdot}xH_2O$, 0.222 g (2.00 × 10^{-3} mol) of SeO_2, and 1 mL of deionized water were combined. Respective reaction mixtures were transferred to Teflon-lined stainless steel autoclaves. Autoclaves were subsequently sealed and heated to 230 °C, held for 4 days, and cooled at a rate of 6 °C h^{-1} to room temperature. After cooling, the autoclaves were opened and the products were recovered by filtration and washed with distilled water. Colorless crystals were

dx.doi.org/10.1021/ic400458a | Inorg. Chem. 2013, 52, 5176−5184

obtained in 32%, 34%, 32%, and 28% yields for $LiGa(SeO_3)_2$, $NaGa(SeO_3)_2$, $KGa(SeO_3)_2$, and $CsGa(SeO_3)_2$, respectively, based on the corresponding alkali-metal carbonates. Powder X-ray diffraction patterns on the ground polycrystalline samples exhibited the materials were single phases and in good agreements with generated patterns from single-crystal data (see the Supporting Information).

Single-Crystal X-ray Diffraction. Structures of $AGa(SeO_3)_2$ (A = Li, Na, K, and Cs) were determined by standard crystallographic methods. A colorless rod (0.013 × 0.025 × 0.049 mm^3) for $LiGa(SeO_3)_2$, a colorless block (0.025 × 0.031 × 0.050 mm^3) for $NaGa(SeO_3)_2$, a colorless block (0.015 × 0.037 × 0.042 mm^3) for $KGa(SeO_3)_2$, and a colorless rod (0.023 × 0.026 × 0.041 mm^3) for $CsGa(SeO_3)_2$ were used for single-crystal data analyses. All of the data were collected using a Bruker SMART BREEZE diffractometer equipped with a 1K CCD area detector using graphite-monochromated Mo Kα radiation at 173 K. A hemisphere of data was collected using a narrow-frame method with scan widths of 0.30° in omega and an exposure time of 5 s/frame. The first 50 frames were remeasured at the end of data collection to monitor instrument and crystal stability. The maximum correction applied to the intensities was <1%. Data were integrated using the SAINT program,[8] with the intensities corrected for Lorentz factor, polarization, air absorption, and absorption attributable to the variation in the path length through the detector faceplate. A semiempirical absorption correction was made on the hemisphere of data with the SADABS program.[9] Data were solved and refined using SHELXS-97[10] and SHELXL-97.[11] All calculations were performed using the WinGX-98 crystallographic software package.[12] Crystallographic data and selected bond distances with bond valence sums for the reported material are given in Tables 1 and 2, respectively.

Powder X-ray Diffraction. The powder X-ray diffraction method has been used to make sure the synthesized materials are pure. Powder XRD data were collected on a Bruker D8-Advance diffractometer using Cu Kα radiation at room temperature with 40 kV and 40 mA. Ground crystalline samples were mounted on sample holders and scanned in the 2θ range 10−70° with a step size of 0.02° and a step time of 0.2 s. Experimental powder XRD patterns are in good agreement with those calculated data from the single-crystal models.

Infrared Spectroscopy. Infrared spectra were recorded on a Varian 1000 FT-IR spectrometer in the 400−4000 cm^{-1} range with the sample embedded in a KBr matrix.

Thermogravimetric Analysis. Thermogravimetric analysis was performed on a Setaram LABSYS TG-DTA/DSC Thermogravimetric Analyzer. Polycrystalline samples were contained within alumina crucibles and heated at a rate of 10 °C min^{-1} from room temperature to 1000 °C under flowing argon.

Scanning Electron Microscopy/Energy-Dispersive Analysis by X-ray (SEM/EDAX). SEM/EDAX has been performed using a Hitachi S-3400N/Horiba Energy EX-250 instruments. EDAX for $NaGa(SeO_3)_2$, $KGa(SeO_3)_2$, and $CsGa(SeO_3)_2$ exhibit A/Ga/Se ratios of 1.0:1.0:1.9, 1.0:1.0:2.1, and 1.0:1.1:2.2, respectively.

Second-Order Nonlinear Optical Measurements. Powder SHG measurements on polycrystalline $LiGa(SeO_3)_2$ were performed on a modified Kurtz-NLO system[13] using 1064 nm radiation. A DAWA Q-switched Nd:YAG laser, operating at 20 Hz, was used for measurements. Because SHG efficiency has been shown to depend strongly on particle size, polycrystalline samples were ground and sieved (Newark Wire Cloth Co.) into distinct particle size ranges (20−45, 45−63, 63−75, 75−90, 90−125, >125 μm). To make relevant comparisons with known SHG materials, crystalline α-SiO_2 and $LiNbO_3$ were also ground and sieved into the same particle size ranges. Powders with particle size 45−63 μm were used for comparing SHG intensities. All powder samples with different particle sizes were placed in separate capillary tubes. No index matching fluid was used in any of the experiments. The SHG light, i.e., 532 nm green light, was collected in reflection and detected by a photomultiplier tube (Hamamatsu). To detect only the SHG light, a 532 nm narrow-pass interference filter was attached to the tube. A digital oscilloscope (Tektronix TDS1032) was used to view the SHG signal. A detailed description of the equipment and methodology used has been published.[14]

RESULTS AND DISCUSSION

Structures. *$LiGa(SeO_3)_2$.* $LiGa(SeO_3)_2$ crystallizes in the noncentrosymmetric tetragonal space group *I*-42*d* (No. 122). The new quaternary lithium gallium selenite exhibits a similar structure to that of $LiFe(SeO_3)_2$ (see Figure 1a).[15] Ga−O bond

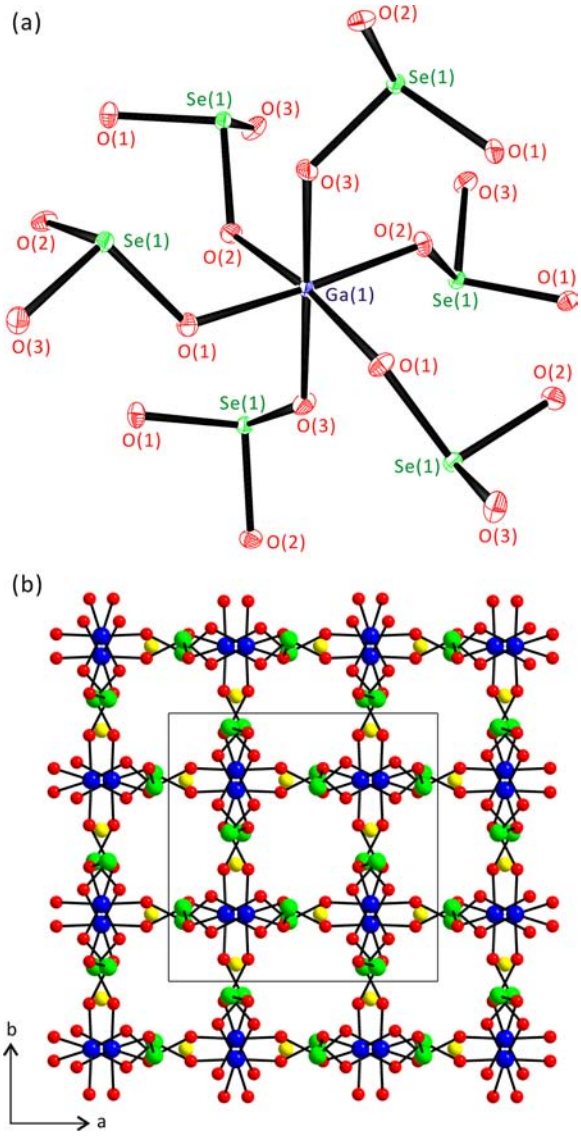

Figure 1. (a) ORTEP (50% probability ellipsoids) drawing representing connections of GaO_6 octahedra and asymmetric SeO_3 polyhedra in $LiGa(SeO_3)_2$. (b) Ball-and-stick model of $LiGa(SeO_3)_2$ representing a three-dimensional framework structure in the *ab* plane (blue, Ga; green, Se; yellow, Li; red, O).

distances range from 1.955(3) to 1.991(3) Å, and O−Ga−O bond angles range from 84.92(13)° to 175.7(2)°. Se^{4+} cations reveal asymmetric coordination environments attributable to the stereoactive nonbonded electron pair. The Se−O bond distances range from 1.682(3) to 1.706(3) Å, and the O−Se−O bond angles range from 98.28(15)° to 100.67(15)°. The Li^+ cation is surrounded by four oxygen atoms with Li−O contact distances ranging from 1.980(10) to 2.001(9) Å. All six oxygen atoms connected to the Ga^{3+} cation are further bonded to a Se^{4+} cation. Also, each oxygen atom linked to the Se^{4+} cation is further shared by the Ga^{3+} cation, which results in a three-dimensional framework structure (see Figure 1b). Thus, in

dx.doi.org/10.1021/ic400458a | Inorg. Chem. 2013, 52, 5176−5184

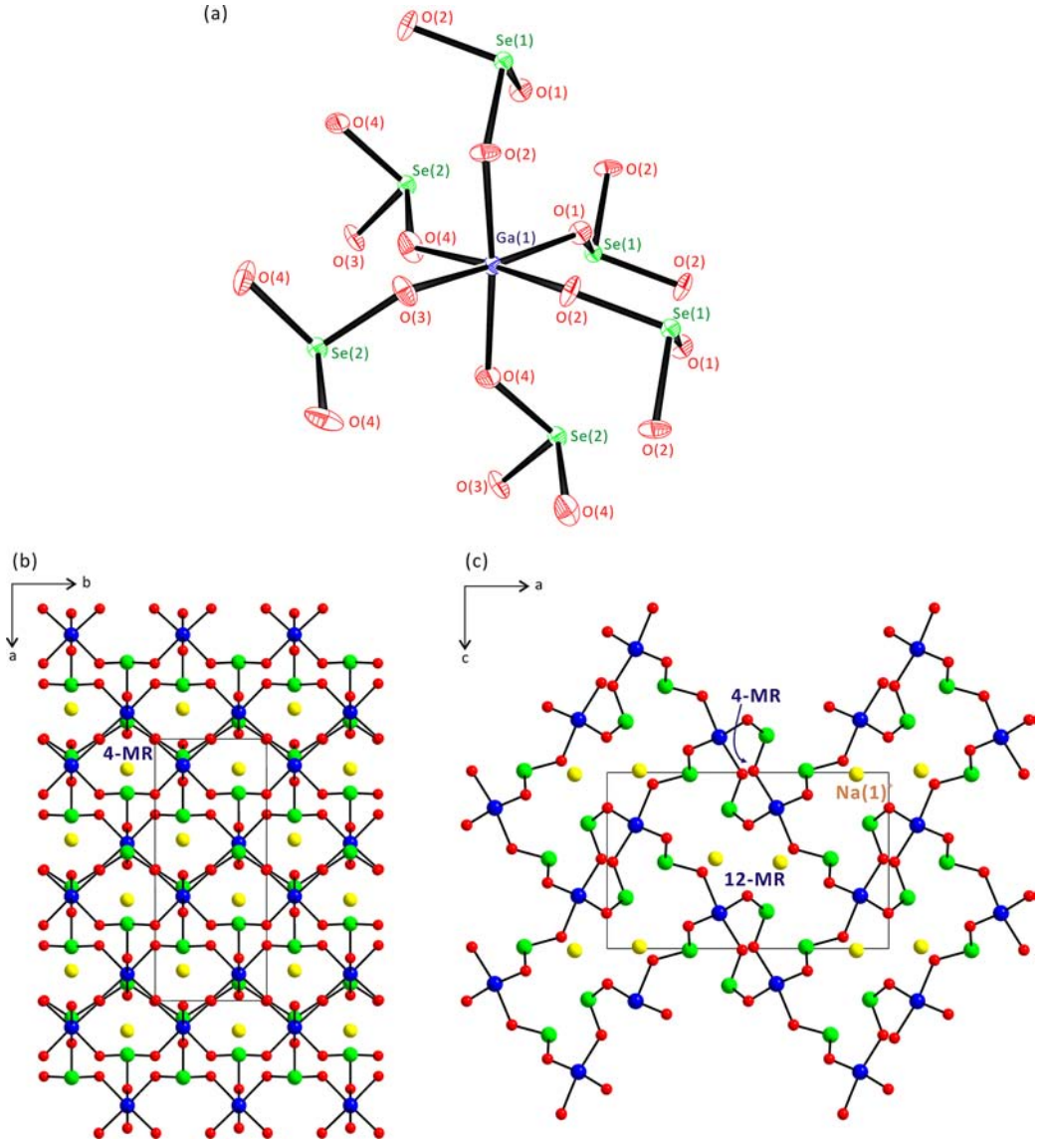

Figure 2. (a) ORTEP (50% probability ellipsoids) drawing representing connections of GaO_6 octahedra and asymmetric SeO_3 polyhedra in $NaGa(SeO_3)_2$. (b) Ball-and-stick model of $NaGa(SeO_3)_2$ in the *ab* plane. Four-membered ring (4-MR) channels running down the [001] direction are observed. (c) Small 4-membered ring channels and large 12-membered ring channels composed of GaO_6 octahedra and SeO_3 polyhedra are observed along the [010] direction in the *ac* plane (blue, Ga; green, Se; yellow, Na; red, O).

connectivity terms, the structure of $LiGa(SeO_3)_2$ can be described as an anionic framework of $\{[GaO_{6/2}]^{3-}2[SeO_{3/2}]^{1+}\}^{-}$. Charge neutrality is maintained by the Li^+ cation. Bond valence calculations[16] for Ga^{3+}, Se^{4+}, Li^+, and O^{2-} result in values 3.01, 3.83, 0.91, and 2.00–2.06, respectively.

$NaGa(SeO_3)_2$. $NaGa(SeO_3)_2$ exhibits a similar structure to that of $NaIn(SeO_3)_2$ (see Figure 2a).[6] While the Ga–O bond lengths in the GaO_6 octahedra range from 1.925(4) to 1.993(3) Å, the O–Ga–O bond angles vary from 83.41(13)° to 173.54(13)°. Se–O bond distances range from 1.678(4) to 1.695(4) Å. Na^+ cation is encompassed by eight oxygen atoms with Na–O contact distances ranging from 2.483(4) to 2.7782(15) Å. $NaGa(SeO_3)_2$ shows a three-dimensional framework structure consisting of corner-shared GaO_6 octahedra and SeO_3 polyhedra. As seen in Figure 2b, four-membered ring (4-MR) channels that are running down the [001] direction are observed in the *ab* plane. Besides, 4- (4-MR) and 12-membered ring (12-MR) channels composed of GaO_6 octahedra and SeO_3 polyhedra are also observed along the [010] direction in the *ac* plane (see Figure 2c). Na^+ cations are residing within the larger 12-MR channels. Lone pairs on the asymmetric SeO_3 groups are pointing inward within the 12-MR channels. In connectivity terms, the structure of $NaGa(SeO_3)_2$ may be described as an anionic framework of $\{[GaO_{6/2}]^{3-}2[SeO_{3/2}]^{1+}\}^{-}$. Charge balance is maintained through the incorporated Na^+ cation. Bond valence calculations[16] for Ga^{3+}, Se^{4+}, Na^+, and O^{2-} result in values of 3.09, 4.12–4.18, 0.92, and 1.96–2.03, respectively.

$KGa(SeO_3)_2$. $KGa(SeO_3)_2$ reveals similar structure to that of $RbIn(SeO_3)_2$ (see Figure 3a).[6] Ga–O bond distances range from 1.956(2) to 2.0181(15) Å, and O–Ga–O bond angles range from 83.73(9)° to 178.40(9)°. Se–O bond lengths for the two unique Se^{4+} cations range from 1.6928(17) to 1.700(2) Å. K^+ cation is surrounded by eight oxygen atoms with K–O contact lengths ranging from 2.8112(17) to 2.9203(10) Å. GaO_6 octahedra and asymmetric SeO_3 polyhedra share their

dx.doi.org/10.1021/ic400458a | *Inorg. Chem.* 2013, 52, 5176–5184

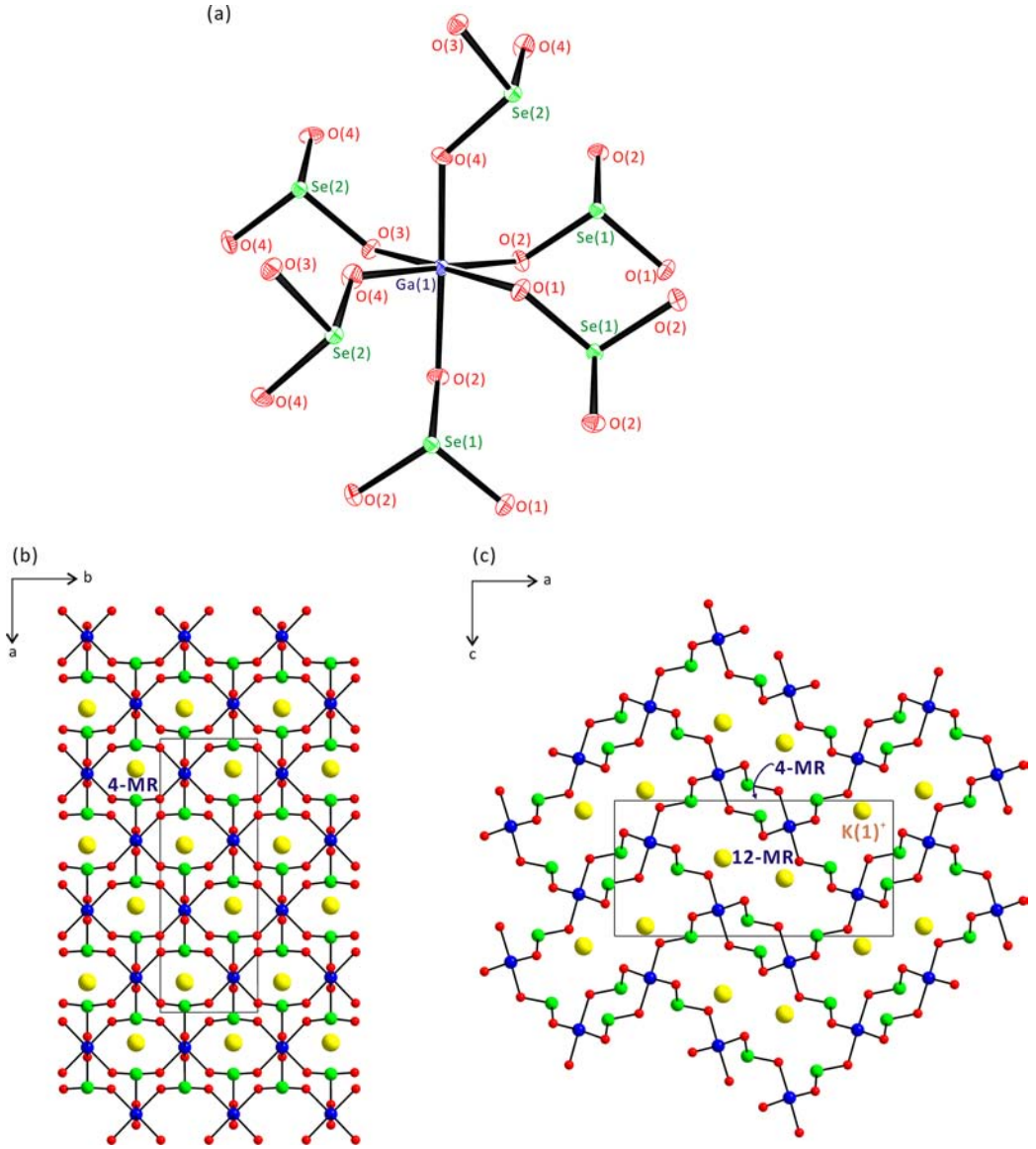

Figure 3. (a) ORTEP (50% probability ellipsoids) drawing representing connections of GaO_6 octahedra and asymmetric SeO_3 polyhedra in $KGa(SeO_3)_2$. (b) Ball-and-stick model of $KGa(SeO_3)_2$ in the *ab* plane. Four-membered ring (4-MR) channels running down the [001] direction are observed. (c) Small 4-membered ring channels and large 12-membered ring channels composed of GaO_6 octahedra and SeO_3 polyhedra are observed along the [010] direction in the *ac* plane (blue, Ga; green, Se; yellow, K; red, O).

corners through oxygen atoms and result in a three-dimensional framework structure (see Figure 3). Although $KGa(SeO_3)_2$ shows a similar channel structure to that of $NaGa(SeO_3)_2$, the framework structures are different from each other (see Figures 3b and 3c). While the lone pairs on the SeO_3 polyhedra in $KGa(SeO_3)_2$ are pointing inward within the 4-MR channels, those in $NaGa(SeO_3)_2$ are all oriented inward within the 12-MR channels. The different framework structures may be attributable to the different sizes of the alkali-metal cations. In connectivity terms, the structure of $KGa(SeO_3)_2$ can be described as an anionic framework of $\{[GaO_{6/2}]^{3-}2\text{-}[SeO_{3/2}]^{1+}\}^{-}$. Charge neutrality is maintained by the K^+ cation. Bond valence calculations[16] for Ga^{3+}, Se^{4+}, K^+, and O^{2-} result in values of 2.98, 4.10−4.11, 1.06, and 1.85−2.01, respectively.

$CsGa(SeO_3)_2$. $CsGa(SeO_3)_2$ is a new three-dimensional quaternary Cs^+−Ga^{3+}−Se^{4+} oxide containing distorted GaO_6 octahedra and asymmetric SeO_3 groups that are connected by Ga−O−Se bonds (see Figure 4a). Within an asymmetric unit, two unique Ga^{3+} cations exist and the Ga−O bond distances range from 1.943(6) to 2.037(6) Å. O−Ga−O bond angles range from 73.7(3)° to 177.6(3)°. Se−O bond lengths range from 1.691(9) to 1.715(8) Å. There are three unique Cs^+ cations, and they are surrounded by 8, 10, and 12 oxygen atoms with Cs−O contact distances ranging from 3.054(6) to 3.632(6) Å. All of the oxygen atoms in the corners of the GaO_6 octahedra are shared by the SeO_3 groups. Then each oxygen atom in the SeO_3 polyhedra is further shared by the GaO_6 octahedra, which completes a three-dimensional framework structure. Coordination modes for the selenite groups in the reported materials are slightly different. In $AGa(SeO_3)_2$ (A = Li, Na, and K), all of the selenite groups share their corners through oxygen atoms with GaO_6 octahedra to form three-dimensional frameworks. However, both corner- and edge-shared SeO_3 groups are observed in $CsGa(SeO_3)_2$. As can be seen in Figure 4b, 4-membered ring (4-MR) channels and two different kinds of 12-membered ring (12-MR) channels

dx.doi.org/10.1021/ic400458a | *Inorg. Chem.* 2013, 52, 5176−5184

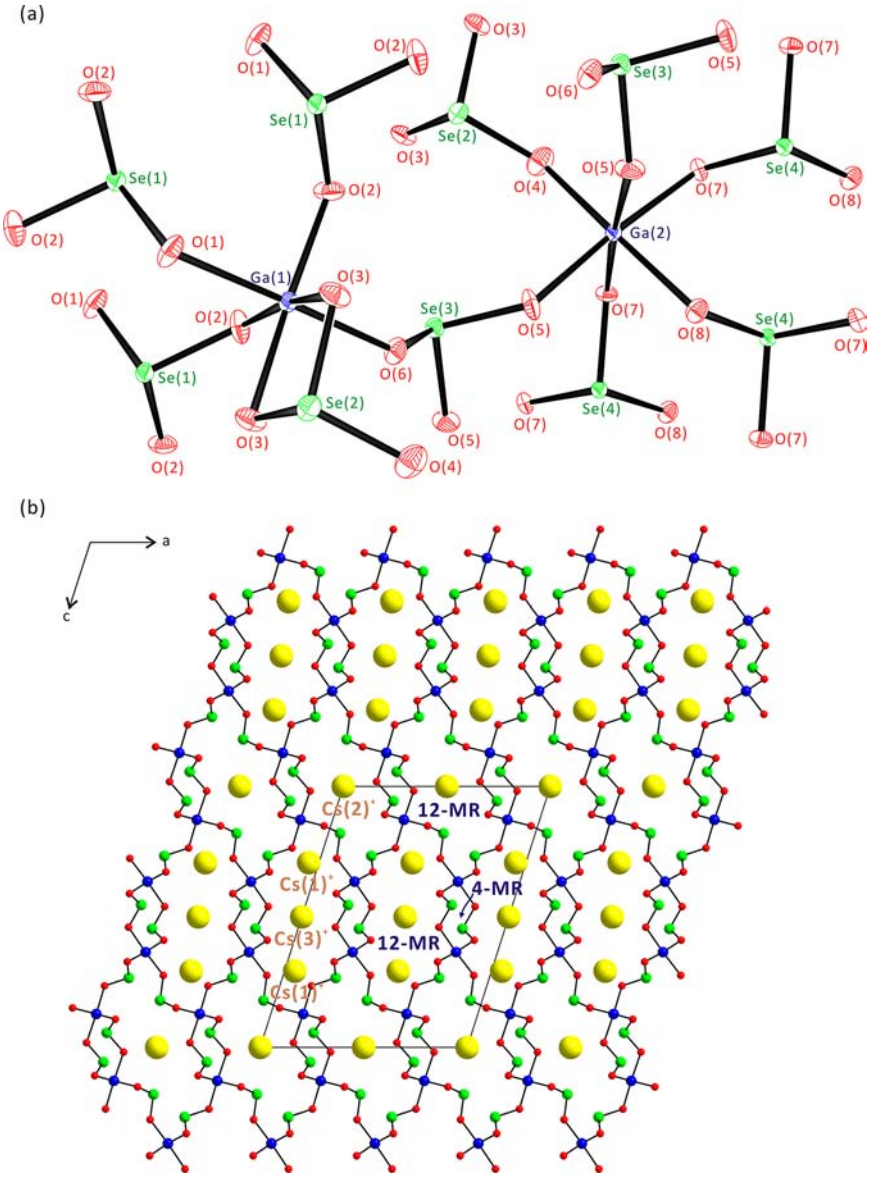

Figure 4. (a) ORTEP (50% probability ellipsoids) drawing representing connections of GaO_6 octahedra and asymmetric SeO_3 polyhedra in $CsGa(SeO_3)_2$. (b) Ball-and-stick model of $CsGa(SeO_3)_2$ in the *ac* plane. Small 4-membered ring channels and two kinds of large 12-membered ring channels composed of GaO_6 octahedra and SeO_3 polyhedra are observed along the [010] direction in the *ac* plane (blue, Ga; green, Se; yellow, Cs; red, O).

consisting of both GaO_6 octahedra and SeO_3 polyhedra are observed along the [010] direction in the *ac* plane. No Cs^+ cations are observed in the smaller 4-MR channels. However, $Cs(1)^+$ and $Cs(3)^+$ cations reside within one 12-MR channels and $Cs(2)^+$ cations dwell within another 12-MR channels. Lone pairs on the SeO_3 polyhedra in $CsGa(SeO_3)_2$ are pointing inward within the 4-MR channels and 12-MR channels with $Cs(2)^+$ cations. In connectivity terms, the structure of $CsGa(SeO_3)_2$ may be described as an anionic framework of $\{[Ga(1)O_{6/2}]^{3-}[Ga(2)O_{6/2}]^{3-}[Se(1)O_{3/2}]^{1+}[Se(2)O_{3/2}]^{1+}[Se(3)O_{3/2}]^{1+}[Se(4)O_{3/2}]^{1+}\}^{2-}$. Charge neutrality is maintained through the Cs^+ cations. Bond valence calculations[16] for Ga^{3+}, Se^{4+}, Cs^+, and O^{2-} result in values in the range of 2.89−2.98, 3.92−4.14, 0.70−1.38, and 1.79−2.08, respectively.

Cation Size and Channel Structures. The reported alkali-metal gallium selenite materials, $AGa(SeO_3)_2$ (A = Li, Na, K, and Cs), are stoichiometrically equivalent, and their frameworks share a similar bonding network. Framework structures of all four materials are composed of distorted GaO_6 octahedra and asymmetric SeO_3 polyhedra with Ga−O−Se bonds, and the alkali-metal cations reside in the respective channels. Once the structures are examined more closely one can find that the size of the alkali-metal cations and the orientation of lone pairs on Se^{4+} cations play important roles in determining the framework architecture. In $CsGa(SeO_3)_2$, as we described earlier, there are two kinds of 12-MR channels as well as 4-MR channels. As can be seen in Figure 5a, the first 12-MR channels contain three huge Cs^+ cations; thus, all of the lone pairs on the SeO_3 groups are pointing outward of the 12-MR channels. Only one Cs^+ cation, however, resides within the other 12-MR channel, in which four lone pairs are pointing inward within the 12-MR channel. Also, the lone pairs within the smaller 4-MR channels are pointing inward. In $KGa(SeO_3)_2$, relatively larger K^+ cations sit and occupy quite a bit of space within the 12-MR channels.

dx.doi.org/10.1021/ic400458a | *Inorg. Chem.* 2013, 52, 5176−5184

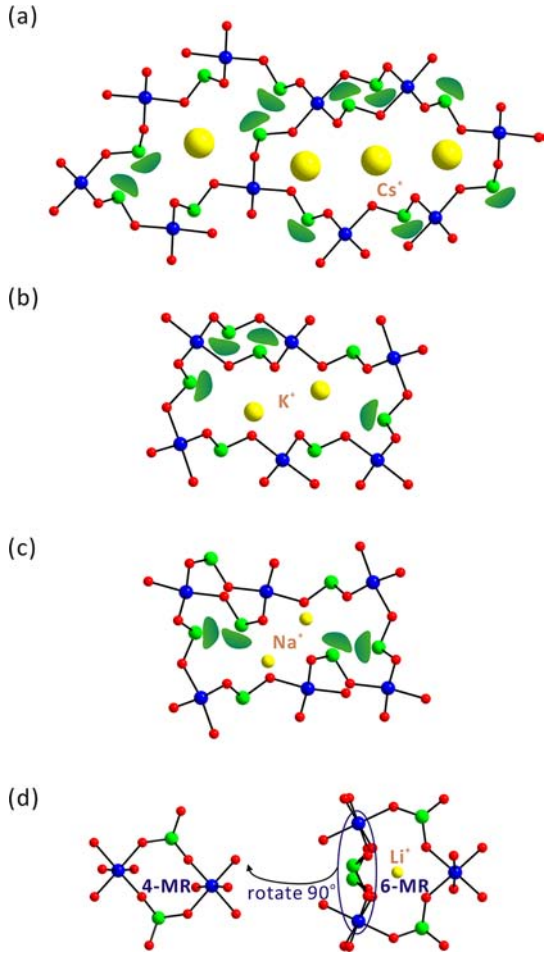

Figure 5. Ball-and-stick representations of the network of GaO_6 octahedra and SeO_3 groups in (a) $CsGa(SeO_3)_2$, (b) $KGa(SeO_3)_2$, (c) $NaGa(SeO_3)_2$, and (d) $LiGa(SeO_3)_2$ (blue, Ga; green, Se; yellow, Cs, K, Na, or Li; red, O). Lone pair on Se^{4+} is drawn schematically and not the result of the electron localization function (ELF) calculations. Note how the size of the alkali-metal cations influences the framework structures.

Thus, two lone pairs on the Se^{4+} cations are oriented inward in the 12-MR channels, and the other lone pairs on the SeO_3 groups are pointing inward within the smaller 4-MR channels (see Figure 5b). In $NaGa(SeO_3)_2$, however, all of the lone pairs on the SeO_3 groups are pointing inward within the larger 12-MR channels. Since the size of the Na^+ cation is relatively small, the channels still possess enough room for the lone pairs (see Figure 5c). Thus far, 4-MR and 12-MR channels are observed from the frameworks of $AGa(SeO_3)_2$ (A = Na, K, and Cs), although their structures are slightly dissimilar. However, in $LiGa(SeO_3)_2$, smaller 4-MRs and 6-MRs are observed in a completely different framework geometry, which is attributable to the much smaller size of the Li^+ cation (see Figure 5d). Interestingly, in $LiGa(SeO_3)_2$, the Li^+ cation is in a distorted tetrahedral coordination environment and interacts strongly with oxide ligands on GaO_6 and SeO_3 groups. In fact, the contact distances for Li^+ cations and oxygen atoms (1.980(10)−2.001(9) Å) are much shorter than those observed from materials with larger cations. In order to keep this tetrahedral environment around the Li^+ cation, the SeO_3 polyhedra are locally aligned. This local alignment of SeO_3 polyhedra prohibits formation of inversion centers and minimizes any unfavorable lone pair−lone pair interactions between the SeO_3 polyhedra. The similar cation size effect on the coordination environment and macroscopic centricities of materials has been observed before from several mixed metal oxides.[5a,b,17] Also, the corresponding coordination environment preference can be confirmed by bond valence calculations. Bond valence sum calculations for the larger cations, Na^+, K^+, and Cs^+, after replacing Li^+ in the $LiGa(SeO_3)_2$ structure result in values of 1.99, 4.16, and 8.73, respectively. Comparing with the bond valence sum for Li^+ (0.91) in the smaller coordination environment, the larger cations are extremely overbonded. In fact, the large cation such as Cs^+ could not easily replace the small Li^+, as the ionic radius of Cs^+ (1.74 Å) is more than twice than that of Li^+ (0.59 Å).

Infrared Spectroscopy. Infrared spectra of $AGa(SeO_3)_2$ (A = Li, Na, K, and Cs) exhibit Ga−O and Se−O vibrations in the region between 410 and 870 cm^{-1}. Bands for Ga−O vibrations are observed around 420−468 cm^{-1}. Multiple bands found between 501 and 869 cm^{-1} are attributable to the Se−O vibrations. Assignments are consistent with those previously reported.[5g,7d,g] Infrared spectra for the reported materials have been deposited in the Supporting Information.

Thermal Analysis. Thermal behaviors of the reported materials have been investigated using thermogravimetric analyses. $AGa(SeO_3)_2$ are thermally stable approximately up to 430 °C based on the TGA diagrams. However, the materials decompose above the temperature attributable to sublimation of SeO_2. Thermal decomposition products at 1000 °C in air for $AGa(SeO_3)_2$ resulted in mixtures of corresponding alkali-metal gallium oxides, $AGaO_2$, and some unknown amorphous phase as confirmed by powder XRD measurements. With $KGa(SeO_3)_2$ or $CsGa(SeO_3)_2$, another alkali-metal gallium oxide phase such as KGa_5O_8 (PDF# 33-1008) or $CsGa_{11}O_{17}$ (PDF# 27−1070), respectively, is also observed from the XRD data. TGA data and powder XRD patterns for the thermally decomposed products have been deposited in the Supporting Information.

Second-Order Nonlinear Optical (NLO) Measurements. Since $LiGa(SeO_3)_2$ crystallizes in a noncentrosymmetric space group, the material's NLO properties have been investigated. Powder SHG measurements, using 1064 nm radiation, indicate that $LiGa(SeO_3)_2$ exhibits SHG efficiency of approximately 5 times that of α-SiO_2. The weak SHG efficiency seems to be attributable to the lack of constructive addition of the dipole moments, which is often found in materials crystallizing in nonpolar space groups. Additional SHG measurements on the sieved polycrystalline $LiGa(SeO_3)_2$ into various particle sizes indicate that the material is not phase matchable (type 1) (see the Supporting Information), with the bulk SHG efficiency, $\langle d_{eff}\rangle_{exp}$, value of approximately 1.2 pm V^{-1}.

Dipole Moment Calculations. All four reported materials include a cation, Se^{4+}, which shows local asymmetric coordination environment attributable to the lone pair. More detailed investigation of materials containing asymmetric lone pair cations certainly enables us to understand better the coordination environments. Thus, we decided to quantify the direction and magnitude of the distortions in the SeO_3 polyhedra by determining the local dipole moments using a method described earlier with respect to octahedra for metal oxyfluorides.[18] The approach uses a bond valence sum to calculate the direction and magnitude of the local dipole moments. With the lone pair polyhedra, the lone pair is given a

dx.doi.org/10.1021/ic400458a | Inorg. Chem. 2013, 52, 5176−5184

charge of −2 and the localized Se^{4+}−lone pair distance is given to be 1.22 Å based on the earlier work of Galy et al.[19] Using this method, the dipole moment for the SeO_3 polyhedra in the reported materials range about from 7.38 to 8.69 D (D = Debyes). The values are consistent with those reported dipole moments for SeO_3 polyhedra.[5e,f,20] The polarizations associated with Se^{4+} completely cancel if the local dipole moments are taken as a whole, which is attributable to the centrosymmetric and/or nonpolar space groups for the reported materials. A complete calculation of dipole moments for the SeO_3 polyhedra is listed in Table 3.

Table 3. Calculation of Dipole Moments for SeO_3 Polyhedra (D = Debyes)

compound	SeO_3	dipole moment (D)
$LiGa(SeO_3)_2$	$Se(1)O_3$	8.34
$NaGa(SeO_3)_2$	$Se(1)O_3$	7.71
	$Se(2)O_3$	8.69
$KGa(SeO_3)_2$	$Se(1)O_3$	8.52
	$Se(2)O_3$	8.03
$CsGa(SeO_3)_2$	$Se(1)O_3$	8.60
	$Se(2)O_3$	7.73
	$Se(3)O_3$	7.38
	$Se(4)O_3$	8.52

CONCLUSIONS

Four new quaternary mixed metal selenite materials, $AGa(SeO_3)_2$ (A = Li, Na, K, and Cs), have been prepared by hydrothermal reactions. All four stoichiometrically equivalent materials exhibit three-dimensional frameworks composed of distorted GaO_6 octahedra and asymmetric SeO_3 polyhedra with Ga−O−Se bonds. However, each of the framework geometries is different depending on the size of the alkali-metal cations. Interactions between the cation and the oxide ligands on GaO_6 and SeO_3 groups also influence determining macroscopic centricities of the materials. Infrared spectroscopy, thermal analysis, dipole moment calculations, and second-harmonic generation properties for the new materials have been obtained.

ASSOCIATED CONTENT

Supporting Information

X-ray crystallographic file in CIF format, calculated and observed X-ray diffraction patterns, thermogravimetric analysis diagrams, infrared spectra, and phase-matching curve for $AGa(SeO_3)_2$ (A = Li, Na, K, and Cs). This material is available free of charge via the Internet at http://pubs.acs.org.

AUTHOR INFORMATION

Corresponding Author

*Phone: +82-2-820-5197. Fax: +82-2-825-4736. E-mail: kmok@cau.ac.kr.

Notes

The authors declare no competing financial interest.

ACKNOWLEDGMENTS

This research was supported by the Basic Science Research Program through the National Research Foundation of Korea (NRF) funded by the Ministry of Education, Science & Technology (grant no. 2010-0002480).

REFERENCES

(1) Halasyamani, P. S.; Poeppelmeier, K. R. *Chem. Mater.* **1998**, *10*, 2753.
(2) (a) Jona, F.; Shirane, G. *Ferroelectric Crystals*; Pergamon Press: Oxford, 1962. (b) Cady, W. G. *Piezoelectricity; an Introduction to the Theory and Applications of Electromechanical Phenomena in Crystals*; Dover: New York, 1964. (c) Lang, S. B. *Sourcebook of Pyroelectricity*; Gordon & Breach Science: London, 1974. (d) Chen, C.; Liu, G. *Annu. Rev. Mater. Sci.* **1986**, *16*, 203. (e) Lines, M. E.; Glass, A. M. *Principles and Applications of Ferroelectrics and Related Materials*; Oxford University Press: Oxford, U.K., 1991. (f) Marder, S. R.; Sohn, J. E.; Stucky, G. D. *Materials for Non-linear Optics: Chemical Perspectives*; American Chemical Society: Washington, DC, 1991. (g) Auciello, O.; Scott, J. F.; Ramesh, R. *Phys. Today* **1998**, *40*, 22. (h) Becker, P. *Adv. Mater.* **1998**, *10*, 979. (i) Keszler, D. A. *Curr. Opin. Solid State Mater. Sci* **1999**, *4*, 155.
(3) (a) Bader, R. F. W. *Mol. Phys.* **1960**, *3*, 137. (b) Bader, R. F. W. *Can. J. Chem.* **1962**, *40*, 1164. (c) Pearson, R. G. *J. Am. Chem. Soc.* **1969**, *91*, 4947. (d) Pearson, R. G. *J. Mol. Struct.: THEOCHEM* **1983**, *103*, 25. (e) Wheeler, R. A.; Whangbo, M.-H.; Hughbanks, T.; Hoffmann, R.; Burdett, J. K.; Albright, T. A. *J. Am. Chem. Soc.* **1986**, *108*, 2222. (f) Kunz, M.; Brown, I. D. *J. Solid State Chem.* **1995**, *115*, 395.
(4) (a) Kepert, C. J.; Prior, T. J.; Rosseinsky, M. J. *J. Am. Chem. Soc.* **2000**, *122*, 5158. (b) Maggard, P. A.; Stern, C. L.; Poeppelmeier, K. R. *J. Am. Chem. Soc.* **2001**, *123*, 7742. (c) Hwu, S.-J.; Ulutagay-Kartin, M.; Clayhold, J. A.; Mackay, R.; Wardojo, T. A.; O'Connor, C. J.; Kraweic, M. *J. Am. Chem. Soc.* **2002**, *124*, 12404. (d) Welk, M. E.; Norquist, A. J.; Arnold, F. P.; Stern, C. L.; Poeppelmeier, K. R. *Inorg. Chem.* **2002**, *41*, 5119. (e) West, J. P.; Hwu, S.-J. *J. Solid State Chem.* **2012**, *195*, 101.
(5) (a) Sykora, R. E.; Ok, K. M.; Halasyamani, P. S.; Albrecht-Schmitt, T. E. *J. Am .Chem. Soc.* **2002**, *124*, 1951. (b) Goodey, J.; Ok, K. M.; Broussard, J.; Hofmann, C.; Escobedo, F. V.; Halasyamani, P. S. *J. Solid State Chem.* **2003**, *175*, 3. (c) Ok, K. M.; Baek, J.; Halasyamani, P. S.; O'Hare, D. *Inorg. Chem.* **2006**, *45*, 10207. (d) Choi, M.-H.; Kim, S.-H.; Chang, H. Y.; Halasyamani, P. S.; Ok, K. M. *Inorg. Chem.* **2009**, *48*, 8376. (e) Lee, D. W.; Oh, S.-J.; Halasyamani, P. S.; Ok, K. M. *Inorg. Chem.* **2011**, *50*, 4473. (f) Oh, S.-J.; Lee, D. W.; Ok, K. M. *Inorg. Chem.* **2012**, *51*, 5393. (g) Lee, D. W.; Bak, D.-b.; Kim, S. B.; Kim, J.; Ok, K. M. *Inorg. Chem.* **2012**, *51*, 7844.
(6) Lee, D. W.; Kim, S. B.; Ok, K. M. *Inorg. Chem.* **2012**, *51*, 8530.
(7) (a) Rastsvetaeva, R. K.; Petrova, G. K.; Andrianov, V. I. *Dokl. Akad. Nauk S.S.S.R.* **1983**, *270*, 882. (b) Rastsvetaeva, R. K.; Andrianov, V. I.; Volodina, A. N. *Dokl. Akad. Nauk S.S.S.R.* **1986**, *291*, 352. (c) Morris, R. E.; Cheetham, A. K. *Chem. Mater.* **1994**, *6*, 67. (d) Ok, K. M.; Halasyamani, P. S. *Chem. Mater.* **2002**, *14*, 2360. (e) Kong, F.; Hu, C.; Hu, T.; Zhou, Y.; Mao, J. G. *Dalton Trans.* **2009**, 4962. (f) Kong, F.; Lin, Q.; Yi, F. Y.; Mao, J. G. *Inorg. Chem.* **2009**, *48*, 6794. (g) Kong, F.; Xu, X.; Mao, J. G. *Inorg. Chem.* **2010**, *49*, 11573. (h) Kong, F.; Li, P.; Zhang, S.; Mao, J. G. *J. Solid State Chem.* **2012**, *190*, 118.
(8) *SAINT, Program for Area Detector Absorption Correction*, version 4.05; Siemens Analytical X-ray Instruments: Madison, WI, 1995.
(9) Blessing, R. H. *Acta Crystallogr., Sect. A: Found. Crystallogr.* **1995**, *A51*, 33.
(10) Sheldrick, G. M.; *SHELXS-97-A program for automatic solution of crystal structures*; University of Goettingen: Goettingen, Germany, 1997.
(11) Sheldrick, G. M.; *SHELXL-97-A program for crystal structure refinement*; University of Goettingen: Goettingen, Germany: 1997.
(12) Farrugia, L. J. *J. Appl. Crystallogr.* **1999**, *32*, 837.
(13) Kurtz, S. K.; Perry, T. T. *J. Appl. Phys.* **1968**, *39*, 3798.
(14) Ok, K. M.; Chi, E. O.; Halasyamani, P. S. *Chem. Soc. Rev.* **2006**, *35*, 710.
(15) Giester, G. *Monatsh. Chem. Verw. Teile Anderer Wiss.* **1994**, *125*, 535.
(16) (a) Brown, I. D.; Altermatt, D. *Acta Crystallogr.* **1985**, *B41*, 244. (b) Brese, N. E.; O'Keeffe, M. *Acta Crystallogr.* **1991**, *B47*, 192.

(17) Chang, H.-Y.; Kim, S.-H.; Ok, K. M.; Halasyamani, P. S. *J. Am. Chem. Soc.* **2009**, *131*, 6865.
(18) (a) Maggard, P. A.; Nault, T. S.; Stern, C. L.; Poeppelmeier, K. R. *J. Solid State Chem.* **2003**, *175*, 25. (b) Izumi, H. K.; Kirsch, J. E.; Stern, C. L.; Poeppelmeier, K. R. *Inorg. Chem.* **2005**, *44*, 884.
(19) Galy, J.; Meunier, G. *J. Solid State Chem.* **1975**, *13*, 142.
(20) (a) Lee, D. W.; Ok, K. M. *Solid State Sci.* **2010**, *12*, 2036. (b) Oh, S.-J.; Lee, D. W.; Ok, K. M. *Dalton Trans.* **2012**, *41*, 2995.